Scanning Tunneling Microscopy Investigation of Ordered Thin Films of Bis(4-dioctadecylamino-phenyl) Squaraine on Highly Oriented Pyrolytic Graphite

M. E. Stawasz[†] and B. A. Parkinson*[,‡]

ATMI, Incorporated, 7 Commerce Drive, Danbury, Connecticut 06810, and Department of Chemistry, Colorado State University, Fort Collins, Colorado 80523

Received July 8, 2003. In Final Form: September 3, 2003

Scanning tunneling microscopy (STM) is used to investigate the two-dimensional (2D) ordered structures of bis(4-dioctadecylamino-phenyl) squaraine (referred to as 18-18HSQ), adsorbed from phenyloctane onto the (0001) surface of highly oriented pyrolytic graphite (HOPG). Nucleation and growth of the 2D ordered structures could be observed on the STM time scale for adsorption from lower concentrations of 18-18HSQ in phenyloctane. A number of polymorphs and multiple-layer structures were formed from both low and high deposition solution concentrations; however, single-layer structures were only observed to form from low concentrations. Growth of layers up to three molecules deep could be observed with STM. Although 18-18HSQ is an achiral molecule, 2D chiral polymorphs were observed. The unit cells of the 2D structures of 18-18HSQ were determined to be coincident with the HOPG lattice.

Introduction

Of central importance to the study of physical molecular ordering at interfaces is the competition between two interactions: adsorbate−adsorbate and adsorbate−substrate. Two-dimensional (2D) self-assembled structures physisorbed at the liquid−solid interface in which adsorbate−adsorbate interactions stabilize and drive the observed molecular order tend to form 2D structures that are related to the solid-state structure of the molecules. Conversely, when adsorbate−substrate interactions dominate, the 2D structures tend to be unlike the solid-state structures. The nature of the forces governing organization on the surface (van der Waals, dipole−dipole, charge transfer, etc.) is determined by the structure of the molecule (its functional groups and geometry), the reactivity of the substrate, and the epitaxial relationship of the adsorbate 2D unit cell to the substrate unit cell.

To better determine the role of the chemical structure of an adsorbate molecule on the interplay between adsorbate−adsorbate and adsorbate−substrate interactions and the resulting 2D ordering, the functionalities of the molecule may be systematically varied while the substrate remains constant. To determine the effect of substrate interaction on the 2D organization, a single molecular structure can be adsorbed on a series of different substrates with similar structures but varying reactivity or on a series of substrates with similar reactivity but differing lattice structures. To probe the strength of interaction of an adsorbate with a particular substrate lattice, the functionalities of the molecule may likewise be varied from groups that have little interaction to those that have a strong interaction with the surface.

Scanning tunneling microscopy (STM) has proven to be especially well suited to investigate molecular ordering on surfaces. The adsorption of molecules onto a conducting or semiconducting surface in either air, liquids, or a vacuum may be observed using this technique. STM is unsurpassed in the determination of local 2D adsorbate structure since in some cases it can resolve features down to the atomic scale. As a result, the influence of the systematic variation of a molecule's functionality, substrate reactivity, and substrate lattice structure on the 2D structure has been studied by STM. Many types of molecules (perylenes,[1−14] porphyrins,[15−27]

[†] ATMI, Inc.
[‡] Colorado State University.

(1) Elings, V.; Wudl, F. *J. Vac. Sci. Technol., A* **1988**, *6*, 412−414.
(2) Ludwig, C.; Gompf, B.; Glatz, W.; Petersen, J.; Eisenmenger, W.; Mobus, M.; Zimmermann, U.; Karl, N. *J. Phys.: Condens. Matter* **1992**, *86*, 397−404.
(3) Ludwig, C.; Gompf, B.; Petersen, J.; Strohmaier, R.; Eisenmenger, W. *Z. Phys. B: Condens. Matter* **1994**, *93*, 365−373.
(4) Freund, J.; Probst, O.; Grafstroem, S.; Dey, S.; Kowalski, K.; Neumann, R.; Woertge, M.; Putlitz, G. z. *J. Vac. Sci. Technol., B* **1994**, *12*, 1914−1917.
(5) Forrest, S. R.; Burrows, P. E.; Haskal, E. I.; So, F. F. *Phys. Rev. B* **1994**, *49*, 11309−11321.
(6) Strohmaier, R.; Ludwig, C.; Petersen, J.; Gompf, B.; Eisenmenger, W. *Surf. Sci.* **1996**, *351*, 292−302.
(7) Seidel, C.; Awater, C.; Liu, X. D.; Ellerbrake, R.; Fuchs, H. *Surf. Sci.* **1997**, *371*, 123−130.
(8) Schmitz-Hubsch, T.; Fritz, T.; Sellam, F.; Staub, R.; Leo, K. *Phys. Rev. B* **1997**, *55*, 7972−7976.
(9) Kendrick, C.; Kahn, A. *J. Cryst. Growth* **1997**, *181*, 181−192.
(10) Strohmaier, R.; Petersen, J.; Gompf, B.; Eisenmenger, W. *Surf. Sci.* **1998**, *418*, 91−104.
(11) Schmitz-Hubsch, T.; Fritz, T.; Staub, R.; Back, A.; Armstrong, N. R.; Leo, K. *Surf. Sci.* **1999**, *437*, 163−172.
(12) Seidel, C.; Schafer, A. H.; Fuchs, H. *Surf. Sci.* **2000**, *459*, 310−322.
(13) Kaneda, Y.; Stawasz, M. E.; Sampson, D. L.; Parkinson, B. A. *Langmuir* **2001**, *17*, 6185−6195.
(14) Nowakowski, R.; Seidel, C.; Fuchs, H. *Phys. Rev. B* **2001**, *6319*, 5418.
(15) Jung, T. A.; Schlittler, R. R.; Gimzewski, J. K.; Tang, H.; Joachim, C. *Science* **1996**, *271*, 181−184.
(16) Jung, T. A.; Schlittler, R. R.; Gimzewski, J. K. *Nature* **1997**, *386*, 696−698.
(17) Wang, H. N.; Wang, C.; Zeng, Q. D.; Xu, S. D.; Yin, S. X.; Xu, B.; Bai, C. L. *Surf. Interface Anal.* **2001**, *32*, 266−270.
(18) Qiu, X. H.; Wang, C.; Zeng, Q. D.; Xu, B.; Yin, S. X.; Wang, H. N.; Xu, S. D.; Bai, C. L. *J. Am. Chem. Soc.* **2000**, *122*, 5550−5556.
(19) Kunitake, M.; Batina, N.; Itaya, K. *Langmuir* **1995**, *11*, 2337−2340.
(20) Fukushima, H.; Taylor, D. M.; Morgan, H. *Langmuir* **1995**, *11*, 3523−3528.
(21) Ogaki, K.; Batina, N.; Kunitake, M.; Itaya, K. *J. Phys. Chem.* **1996**, *100*, 7185−7190.
(22) Kunitake, M.; Akiba, U.; Batina, N.; Itaya, K. *Langmuir* **1997**, *13*, 1607−1615.
(23) Thomas, P. J.; Berovic, N.; Laitenberger, P.; Palmer, R. E.; Bampos, N.; Sanders, J. K. M. *Chem. Phys. Lett.* **1998**, *294*, 229−232.

10.1021/la035238q CCC: $25.00
Published on Web 00/00/0000 PAGE EST: 12.4

and phthalocyanines[4,5,18,28−43]) have been studied in this way, but the investigations of the substituted alkanes[44−63] have been the most systematic.

The surface structure and ordering of squaraine dyes have not been extensively studied or imaged with STM. Thin films of squaraines are used industrially as photoconductors in photocopiers and laser printers. Their interfacial and subsequent three-dimensional (3D) ordering in the thin film photoconductors is important for optimal device performance.[64] A generic squaraine structure is shown below:

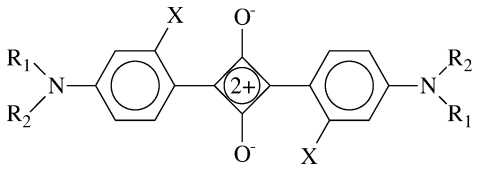

We have previously used STM to study the forces governing the 2D ordering of bis(dialkylamino-hydroxyphenyl) squaraines (OHSQs) and bis(dialkylamino-phenyl) squaraines (HSQs) on a relatively inert substrate, highly oriented pyrolytic graphite (HOPG).[65] Many structural variations can be used to investigate the nature of the forces governing the molecular organization of squaraines on surfaces. The identity and length of the amine substituents can be changed. For example, these substituents are commonly alkyl groups whose length and symmetry can be changed, ($R_1 = R_2$) or ($R_1 \neq R_2$). The identity and position of the phenyl ring substituent (X) of the molecule can also be changed. We have previously investigated the effect of alkyl tail length on the adsorbate−adsorbate interactions and the adsorbate−substrate interactions in a series of symmetric hydroxylated squaraines (OHSQ) adsorbed on HOPG.[65] It was found that the alkyl tail length did cause a shift from herringbone-like structures at short lengths (≤4 carbons) to row structures at longer lengths (≥8 carbons). Herringbone structures appeared to be dominated by donor−acceptor interactions between the chromophores of the adsorbed squaraines. The influence of hydrogen-bonding in forming the structures was not clear, however. Row structures were a result of the increasing influence of tail interactions, both between other tails, via interdigitation, and between the tails and the substrate. The importance of these tail interactions increased as the length of the alkyl tail was increased, resulting in a change from herringbone to J-aggregate-like row structures on the HOPG surface. Even at the longest tail lengths (12 carbons), donor−acceptor interactions were still present in the J-like structures. An epitaxial relationship between the squaraine 2D unit cells and the HOPG surface was not observed, although some tendency toward epitaxy was seen at longer tail lengths.[65]

As mentioned above, the role of the hydroxyl substituent on the phenyl ring and its possible involvement in hydrogen-bonding between adjacent adsorbed molecules was not clear from the investigations of different alkyl tail lengths.[65] To elucidate the role of the hydroxyl substituent, a second series of symmetric HSQs of varying tail lengths adsorbed on HOPG were studied.[66] Many of these molecules were the non-hydroxyl-substituted analogues to the OHSQs discussed above, and thus their 2D structures could be directly compared. It was found that the 2D structures of the OHSQ and HSQ analogues were very much the same, allowing us to conclude that the hydroxyl group on the phenyl ring plays a minimal role in the 2D organization of dialkylamino-phenyl squaraines.[66]

The effect of the symmetry of the squaraine molecule was also investigated. Several HSQ and OHSQ molecules containing two short tails (CH_3 or C_2H_5) and two longer tails (C_6H_{13}, C_8H_{17}, or $C_{18}H_{37}$), one on each side of the

(24) Sashikata, K.; Sugata, T.; Sugimasa, M.; Itaya, K. *Langmuir* **1998**, *14*, 2896−2902.
(25) Bampos, N.; Woodburn, C. N.; Welland, M. E.; Sanders, J. K. M. *Angew. Chem., Int. Ed.* **1999**, *38*, 2780−2783.
(26) Scudiero, L.; Barlow, D. E.; Hipps, K. W. *J. Phys. Chem. B* **2000**, *104*, 11899−11905.
(27) Wan, L. J.; Shundo, S.; Inukai, J.; Itaya, K. *Langmuir* **2000**, *16*, 2164−2168.
(28) Gimzewski, J. K.; Stoll, E.; Schlittler, R. R. *Surf. Sci.* **1987**, *181*, 267−277.
(29) Hamann, C.; Laiho, R.; Mrwa, A. *Phys. Status Solidi A* **1989**, *116*, 729−734.
(30) Ludwig, C.; Strohmaier, R.; Petersen, J.; Gompf, B.; Eisenmenger, W. *J. Vac. Sci. Technol., B* **1994**, *12*, 1963−1966.
(31) Rochet, F.; Dufour, G.; Roulet, H.; Motta, N.; Sgarlata, A.; Piancastelli, M. N.; Decrescenzi, M. *Surf. Sci.* **1994**, *319*, 10−20.
(32) Fritz, T.; Hara, M.; Knoll, W.; Sasabe, H. *Mol. Cryst. Liq. Cryst.* **1994**, *252*, 561−570.
(33) Kanai, M.; Kawai, T.; Motai, K.; Wang, X. D.; Hashizume, T.; Sakura, T. *Surf. Sci.* **1995**, *329*, L619−L623.
(34) Maeda, Y.; Matsumoto, T.; Kasaya, M.; T, T. K. *Jpn. J. Appl. Phys.* **1996**, *35*, L405−L407.
(35) Lu, X.; Hipps, K. W.; Wang, X. D.; Mazur, U. *J. Am. Chem. Soc.* **1996**, *118*, 7197−7202.
(36) Tanaka, H.; Kawai, T. *Jpn. J. Appl. Phys.* **1996**, *35*, 3759−3763.
(37) Lu, X.; Hipps, K. W. *J. Phys. Chem. B* **1997**, *101*, 5391−5396.
(38) Irie, S.; Hoshino, A.; Kuwamoto, K.; Isoda, S.; Miles, M. J.; Kobayashi, T. *Appl. Surf. Sci.* **1997**, *114*, 310−315.
(39) Ottaviano, L.; DiNardo, S.; Lozzi, L.; Passacantando, M.; Picozzi, P.; Santucci, S. *Surf. Rev. Lett.* **1997**, *4*, 59−64.
(40) Ohmori, T.; Masuda, H.; Shimura, M.; Kuroda, J.; Okumura, T. *Thin Solid Films* **1998**, *315*, 1−4.
(41) Smolenyak, P.; Peterson, R.; Nebesny, K.; Torker, M.; O'Brien, D. F.; Armstrong, N. R. *J. Am. Chem. Soc.* **1999**, *121*, 8628−8636.
(42) Barlow, D. E.; Hipps, K. W. *J. Phys. Chem. B* **2000**, *104*, 5993−6000.
(43) Walzer, K.; Hietschold, M. *Surf. Sci.* **2001**, *471*, 1−10.
(44) McGonigal, G. C.; Bernhardt, R. H.; Thomson, D. J. *Appl. Phys. Lett.* **1990**, *57*, 28−30.
(45) Rabe, J. P.; Buchholtz, S. *Science* **1991**, *253*, 424−427.
(46) Watel, G.; Thibaudau, F.; Cousty, J. *Surf. Sci.* **1993**, *281*, L297.
(47) Liang, W.; Whangbo, M.-H.; Wawkuschewski, A.; Cantow, H. J.; Magonov, S. N. *Adv. Mater.* **1993**, *5*, 817.
(48) Wawkuschewski, A.; Cantow, H.-J.; Magonov, S. N.; Moller, M.; Liang, W.; Whangbo, M.-H. *Adv. Mater.* **1993**, *5*, 821−826.
(49) Rabe, J. P.; Buchholz, S.; Askadskaya, L. *Synth. Met.* **1993**, *54*, 339−349.
(50) Venkataraman, B.; Breen, J. J.; Flynn, G. W. *J. Phys. Chem.* **1995**, *99*, 6608−6619.
(51) Hibino, M.; Sumi, A.; Hatta, I. *Jpn. J. Appl. Phys.* **1995**, *34*, 3354.
(52) Stabel, A.; Dasaradhi, L.; O'Hagan, D.; Rabe, J. P. *Langmuir* **1995**, *11*, 1427.
(53) Venkataraman, B.; Flynn, G. W.; Folkers, J. P.; Whitesides, G. M. *J. Phys. Chem.* **1995**, *99*, 8684−8689.
(54) Cyr, D.; Venkataraman, B.; Flynn, G. W.; Black, A.; Whitesides, G. M. *J. Phys. Chem.* **1996**, *100*, 13747−13759.
(55) Takeuchi, H.; Kawauchi, S.; Ikai, A. *Jpn. J. Appl. Phys.* **1996**, *35*, 3754−3758.
(56) Claypool, C. L.; Faglioni, F.; Goddard, W. A., III; Gray, H. B.; Lewis, N. S.; Marcus, R. A. *J. Phys. Chem. B* **1997**, *101*, 5978−5995.
(57) Hibino, M.; Sumi, A.; Tsuchiya, H.; Hatta, I. *J. Phys. Chem. B* **1998**, *102*, 4544−4547.
(58) Lee, H. S.; Iyengar, S.; Musselman, I. H. *Langmuir* **1998**, *14*, 7475−7483.
(59) DeFeyter, S.; Grim, P. C. M.; Esch, J. v.; Kellogg, R. M.; Feringa, B. L.; DeSchryver, F. C. *J. Phys. Chem. B* **1998**, *102*, 8981−8987.
(60) Fang, H.; Giancarlo, L. C.; Flynn, G. W. *J. Phys. Chem. B* **1999**, *103*, 5712−5715.
(61) Claypool, C.; Faglioni, F.; Matzger, A. J.; Goddard, W. A., III; Lewis, N. S. *J. Phys. Chem. B* **1999**, *103*, 9690−9699.
(62) LePoulennec, C.; Cousty, J.; Xie, Z. X.; Mioskowski, C. *Surf. Sci.* **2000**, *448*, 93−100.
(63) Giancarlo, L. C.; Flynn, G. W. *Acc. Chem. Res.* **2000**, *33*, 491−501.
(64) Law, K. Y. *J. Phys. Chem.* **1988**, *92*, 4226−4231.
(65) Stawasz, M. E.; Sampson, D. L.; Parkinson, B. A. *Langmuir* **2000**, *16*, 2326−2342.
(66) Stawasz, M. E.; Parkinson, B. A. Manuscript in preparation.

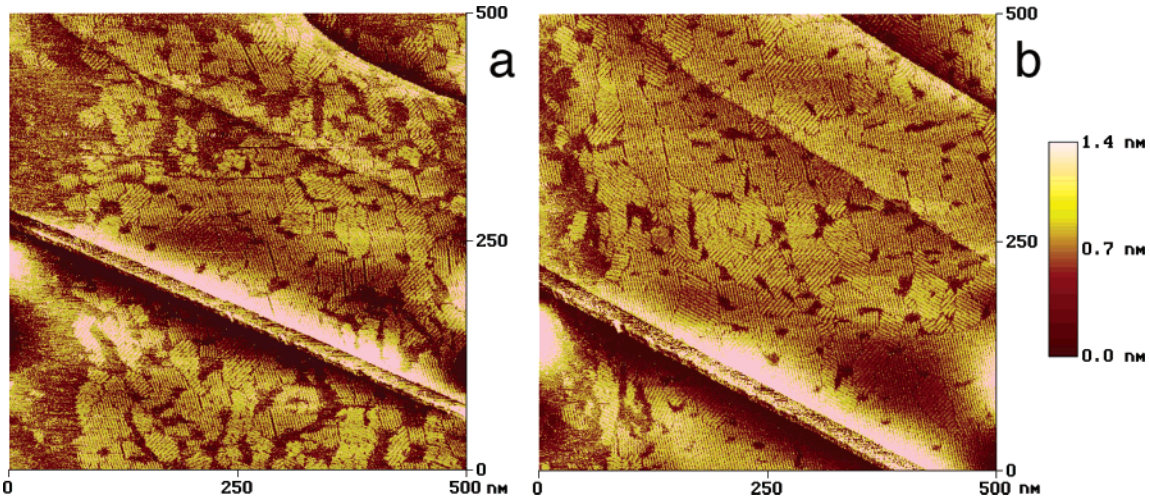

Figure 1. Two sequential 500 nm × 500 nm images showing the ordered adsorption of 18-18HSQ at low deposition solution concentrations. (a) Image captured within seconds of solution deposition. (b) Image captured 9 min after image a.

molecule, were adsorbed onto the surface of HOPG.[65,66] In the case of the squaraines with two methyl tails, the 2D adsorbed structure was the same as that for the more symmetric molecules with all longer tails (i.e., 1-8HSQ and 8-8HSQ/8-8OHSQ). An intriguing effect was observed for the 2D ordering of a less-symmetric OHSQ having one very long tail ($C_{18}H_{37}$) and one short tail (C_2H_5) on each side (2-18OHSQ). It has been observed that long-chain hydrocarbons adsorb lying parallel to the [01$\bar{1}$0] vector on the graphite surface.[67] This has been attributed to the zigzag C backbone along the [01$\bar{1}$0] HOPG lattice vector having very similar C−C−C angles and distances to those of hydrocarbon chains resulting in an epitaxial relationship.[44,45,67,68] It was expected that 2-18OHSQ would experience a similar strong alignment of its long (18 carbons) alkyl tails along this graphite direction. Domains consisting of rigidly straight rows exhibiting intersection angles of 60°, or multiples thereof, were expected. Instead, rows that curved and meandered across the surface, exhibiting no strict relationship to graphite lattice directions, were observed. It was hypothesized that the two short tails (one ethyl on either side of the molecule), instead of four long octadecyl tails, allowed the 2-18OHSQ molecule some flexibility to adsorb and pack on the surface.

The subject of this paper is the 2D ordering of 18-18HSQ on HOPG. The increase in the bulkiness of the molecule, due to adding two additional $C_{18}H_{37}$ tails when compared to 2-18OHSQ, should have implications on the 2D mobility of the molecules on the surface and influence any epitaxial relationship of the ordered overlayer to the HOPG substrate.

Experimental Section

Experiments were performed with a Digital Instruments Nanoscope IIIa STM under ambient conditions. Vibration isolation was provided by a bungee system enclosed within an environmental chamber. Bis(4-dioctadecylamino-phenyl) squaraine (18-18HSQ) was obtained from Dr. Marina Stanescu of the Whitten group at the University of Rochester. Table 1 shows the structure of 18-18HSQ.

Solutions of 18-18HSQ were prepared in concentrations of approximately 10^{-4} to 10^{-6} M in phenyloctane (Aldrich). Experiments were performed with solutions in either the low-concentration range (high 10^{-7} M to low 10^{-5} M) or the high range (high 10^{-5} M to high 10^{-4} M) to observe differences in surface nucleation. STM tips were cut to a sharp point mechanically from 0.2 mm diameter (80:20) platinum/iridium wire (Alpha Aesar). Samples were prepared by applying a drop of squaraine solution onto a freshly cleaved piece of HOPG. Tunneling occurred with the tip immersed into the layer of solution using typical tunneling parameters of −1.6 to −0.8 V (sample negative) and 30 to 45 pA with the scanning tunneling microscope operating in constant current mode. After a series of squaraine images were obtained, the tunneling gap resistance was lowered in order to determine the orientation of the HOPG surface in the exact same spot. Images were obtained with different Pt/Ir tips and several different solutions to test for reproducibility and ensure that the data were free of tip and sample artifacts. All images presented here have been flattened by software routines.

Results and Discussion

Low-Concentration Studies. Two concentration ranges of 18-18HSQ in phenyloctane were investigated: high (high 10^{-5} M to high 10^{-4} M) and low (high 10^{-7} M to low 10^{-5} M). Previous studies demonstrated that squaraines with long alkyl tails tend to form multiple layers of molecules on the HOPG surface.[65] Therefore, STM experiments were performed at low concentrations in an effort to observe nucleation and growth events for single-layer structures and eventual formation of multiple-layer structures.

An STM image obtained within seconds of solution deposition, showing scattered nuclei of molecular domains of 18-18HSQ on the HOPG surface, can be seen in Figure 1a. A subsequent image (Figure 1b), taken 9 min later, shows these islands growing into domains that eventually cover the surface. These domains are composed of alternating bright and dark lamellae or rows. Previous studies[65] of hydroxylated squaraines showed that the chromophore (anilines and four-membered ring) of each adsorbed squaraine molecule is commonly resolved by STM as an oval or "football" shape of bright contrast. The alkyl tails are usually not resolved, however, and appear as dark areas in the image. Measurements of the row spacings of the bright and dark rows shown in Figure 1 reveal that the domains are composed of only one 2D polymorph, designated polymorph 1. This polymorph was observed most frequently in our experiments. The width of the bright rows (measured perpendicular to the edge of the bright row) is ∼19 Å, a larger distance than the length of one 18-18HSQ chromophore measured from N to N (∼14 Å). This suggests, as was often seen in polymorphs formed by other long-tailed squaraines,[65] that

(67) Groszek, A. J. *Proc. R. Soc. London, Ser. A* **1970**, *314*, 473−498.
(68) Watel, G.; Thibaudau, F.; Cousty, J. *Surf. Sci. Lett.* **1993**, *281*, L297−L302.

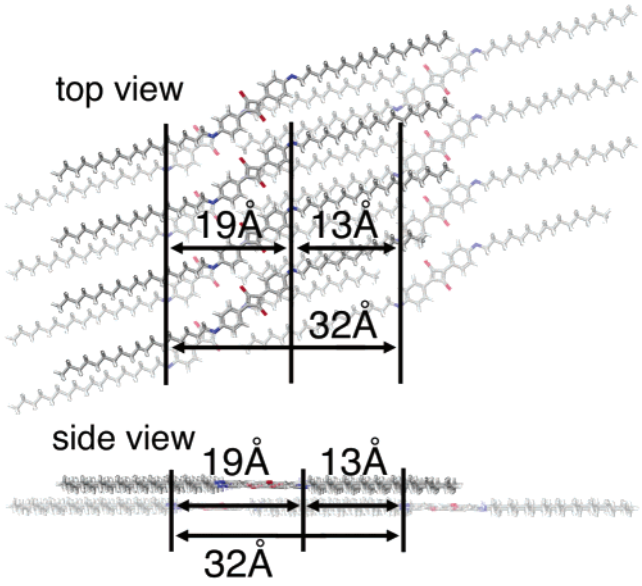

Figure 2. Top and side views of the proposed two-layer molecular model for polymorph 1. The bottom (first) layer is shown shadowed, and the top (second) layer is shown highlighted. The bright row area corresponds to regions occupied by chromophores, whereas the dark row area corresponds to regions occupied only by tails. Arrows indicate the distances corresponding to the *a* unit cell parameter (32 Å), bright row width (19 Å), and dark row width (13 Å).

polymorph 1 consists of multiple layers of chromophores. The dark row width for polymorph 1 is ~14 Å, shorter than the length of an all-trans octadecyl tail (~21 Å), also supporting the model where multiple molecular layers are formed. In the models proposed for other multiple-layer squaraine polymorphs, the second layer of molecules lies on top of the first layer such that the donor and acceptor groups of the bottom and top molecules are aligned but offset from the end of the bottom molecule (the top molecule does not completely eclipse the bottom molecule). The total length of the chromophore region, from the exposed edge of the bottom layer chromophore to the opposite edge of the top chromophore, corresponds to the observed width of the bright row in this polymorph. Because a portion of the tail region of the bottom layer molecules is eclipsed by the top layer chromophores, the dark row width is observed to be less than the actual length of the 18 carbon tails. This configuration is shown in Figure 2.

Coiling or stacking of the 18 carbon tails, due to incorporation of gauche defects, could also explain the observed shortened tail length. We believe these are unlikely, especially in the bottom layer of molecules, due to the attractive interaction of the tails with the HOPG substrate and no previous observations of such effects with other molecules containing long-chain alkyl tails, such as alkylated-perylenes,[13] -phthalocyanines,[18,69] and -porphyrins.[18] The orientation of the chromophores in relation to the edge of the bright molecular rows of polymorph 1 has not been experimentally determined due to insufficient resolution of the images. However, the model shown in Figure 2 was constructed taking into consideration the average angular orientation (~50°) of the chromophores of other long-tailed squaraines that form rows.[65] Likewise, the distance between adjacent chromophores within the same molecular row was not determined. Again, due to the consistency of the ~8 Å distance between adjacent chromophores in all row-forming squaraine 2D structures studied thus far,[65] this distance was used to construct the model shown in Figure 2. It appears that good molecular resolution is hindered by the formation of multiple layers of squaraine molecules, perhaps due to multiple electron tunneling paths to the substrate.

Figure 3a shows a 200 nm by 200 nm STM image of a surface displaying several domains. Measurement of the row widths within these domains has shown that they consist of polymorph 1, just described, and another polymorph (polymorph 2), the second most frequently observed polymorph. Compared to polymorph 1, polymorph 2 has wider dark rows (~33 Å for polymorph 2 vs ~13 Å for polymorph 1) and a larger *a* unit cell parameter (~50 Å vs ~32 Å).

The large dark row width exhibited by polymorph 2 is ~12 Å longer than the length of an all-trans octadecyl tail. We ascribe this to an adsorbed structure with incomplete interdigitation of the octadecyl tails between adjacent molecular rows. The molecular models in Figure 3b,c show that the ~33 Å dark row width corresponds to an overlap of ~6 carbon atoms. The bare areas of graphite created by this incomplete interdigitation are occupied by the remaining two alkyl tails of each molecule, provided that they incorporate several gauche defects, decreasing the tail's observed length. The models in Figure 3b,c show that gauche defects result in the tails twisting out of the plane of the chromophore but then returning to the surface, fitting into the space between interdigitated tails. Although this structure has decreased dispersion interactions between tails in adjacent rows, relative to the fully interdigitated structures, it has increased overall attractive dispersion interactions due to the adsorption onto the HOPG surface of the two usually surface-excluded tails. The energetic cost (the energy difference between the anti and gauche conformations of *n*-butane is ~0.8 kcal/mol[70,71]) of the incorporation of gauche defects (~5 × 0.8 kcal mol^{-1} ≈ 4 kcal mol^{-1}) into the tails to form this structure is outweighed by the larger number of attractive methylene−HOPG interactions now possible (~1.5 kcal mol^{-1} CH_2^{-1} × ~12 CH_2 $tail^{-1}$ ≈ 18 kcal mol^{-1} $tail^{-1}$).[67,72] There is also an additional attractive lateral dispersion interaction between the two tails on each side of every adsorbed chromophore. Solvation energies for the dye in phenyl octane and for displacement of phenyl octane from the graphite surface will also play a role. However, we believe that since the dye is not very soluble in phenyloctane and phenyloctane does not form ordered structures on graphite, these terms are unimportant and to some extent compensating. The bright row width of polymorph 2 (~17 Å) is within experimental error of that of polymorph 1 and, like polymorph 1, consists of two chromophores (oriented at ~50° to the direction of the molecular row) layered atop one another in a way that allows for donor−acceptor interactions.

The asterisks on the STM image in Figure 3a designate areas where polymorphs 1 and 2 coexist. This coexistence can be understood by comparing the dimensions of polymorphs 1 and 2. The *a* unit cell parameter of polymorph 1 (~32 Å) is within experimental error of the dark row width of polymorph 2 (~33 Å). Therefore, the whole structure of polymorph 1 can fit nicely into the area occupied by the tails in polymorph 2. Rather than lying on top of the tails, however, the polymorph 1 structure

(69) Qiu, X.; Wang, C.; Yin, S.; Zheng, Q.; Xu, B.; Bai, C. *J. Phys. Chem. B* **2000**, *104*, 3570−3574.
(70) Szasz, G. J.; Sheppard, N.; Rank, D. H. *J. Chem. Phys.* **1948**, *16*, 704−711.
(71) Woller, P. B.; Garbisch, E. W. *J. Am. Chem. Soc.* **1972**, *94*, 5310.
(72) Kiselev, A. *Russ. J. Phys. Chem.* **1961**, *35*, 111.

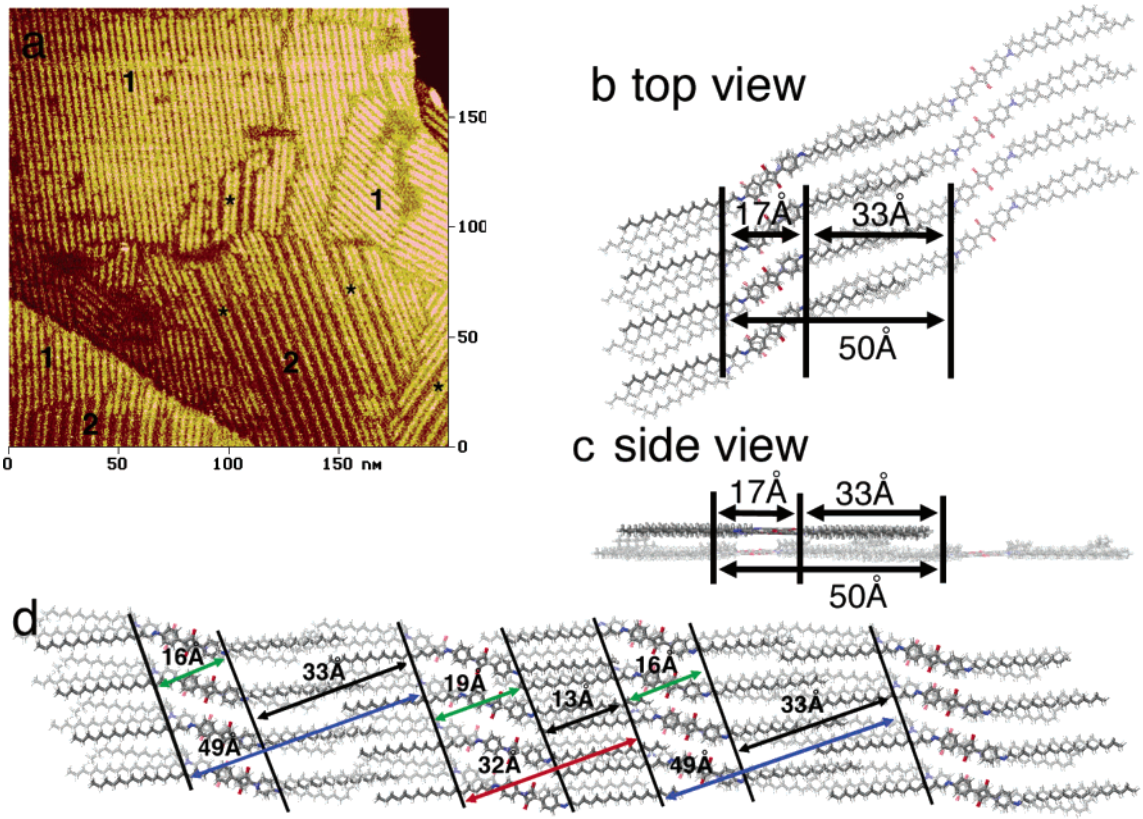

Figure 3. (a) 200 nm × 200 nm STM image showing various domains of polymorphs 1 and 2. Numbers overlaid on the domains identify each polymorph. Asterisks denote areas of polymorph 1 coexisting with areas of polymorph 2. (b) Top and (c) side views of the proposed two-layer molecular model for polymorph 2. (d) Proposed molecular model for incorporation of polymorph 1 into polymorph 2. The bottom (first) layer is shown shadowed, and the second layer is shown highlighted. Bright and dark row widths for polymorphs 1 and 2 are illustrated by green and black double-headed arrows, respectively. The *a* unit cell parameter is designated by a red double-headed arrow for polymorph 1 and a blue arrow for polymorph 2. The *b* unit cell parameter is assumed to be ~8 Å, and $\alpha \sim 90°$.

can incorporate into the tail region. This is shown in the model in Figure 3d. There are two requirements for coexistence of polymorph 1 and 2 within the same domain; each is illustrated in Figure 3d. The first is that the tails adsorbed on the left side of the polymorph 2 row model (16 Å wide bright row), that normally incorporate gauche defects to fit onto the surface, must desorb to allow the more extensive interdigitation of tails within a 13 Å wide dark row of polymorph 1. The second is that the tails on the right side of the polymorph 1 row (19 Å wide bright row), that are normally desorbed, must adsorb onto the surface to make up the energy loss from decreased tail interdigitation within a 34 Å wide dark row. As a result of these alterations, illustrated by asterisks in Figure 3a, a 13 Å polymorph 1 dark row can exist within a domain of polymorph 2 rows.

Figure 4a shows a second type of nucleation observed in STM images, obtained within 1 min of applying low concentrations of the squaraine-containing solution to the freshly cleaved HOPG surface, where there are isolated domains of ordered 18-18HSQ molecules. The area surrounding the domains appears to be occupied by a disordered layer of adsorbed molecules or rapidly moving adsorbed molecules rather than bare graphite as was observed in Figure 1a. (Bare graphite appears very smooth in STM images, whereas areas with disordered molecules appear noisy or fuzzy.) In addition, the size of the domains (~150 nm in diameter) is considerably larger than those observed in Figure 1a (~40 nm). Figure 4b shows an image obtained ~4 min after that in Figure 4a showing domain growth. Zooming in (Figure 4c) reveals that the domains consist of at least two different polymorphs. These polymorphs are distinct from polymorphs 1 and 2 and are labeled 3 and 4 on the image. Holes in the disordered material reveal the bare HOPG surface. It appears that the ordered domains grow by incorporating the disordered adsorbed material.

Higher resolution STM images (Figure 4d), where the chromophores are resolved, were obtained by zooming in on a domain of polymorph 4. Rows of chromophores, where the distance measured from the right edge of one row to the right edge of the next row of chromophores (the *a* unit cell parameter) is 39 ± 1 Å, are seen. The measured width, taken perpendicular to the edges of the rows, of the dark and bright rows is 26 ± 3 Å and 13 ± 2 Å, respectively. The fuzzy stripe appearing to the left of most of the rows of chromophores is possibly due to a second layer of mobile chromophores in the process of adsorbing atop the single-layer polymorph 4 rows that will eventually result in one of the two-layer polymorphs. The fuzzy stripe did not appear in all of the high-resolution images of polymorph 4. The ~13 Å bright row width and the ~15 Å length from end to end of the bright ovals composing the bright rows correspond well to the length of a single squaraine chromophore. The distance between chromophores adjacent to one another in the same row is ~9 Å. The ~26 Å dark row width corresponds to a structure where two of the octadecyl tails (one from each side of the molecule) are adsorbed on the surface interdigitated with the alkyl tails of the molecules in the row adjacent to it. This interdigitation is not complete, however. The dark rows are 5−6 Å longer than a single octadecyl tail (~20 Å), meaning that ~3 of the methylene groups from each adsorbed tail are not interdigitated. The molecular model shown in

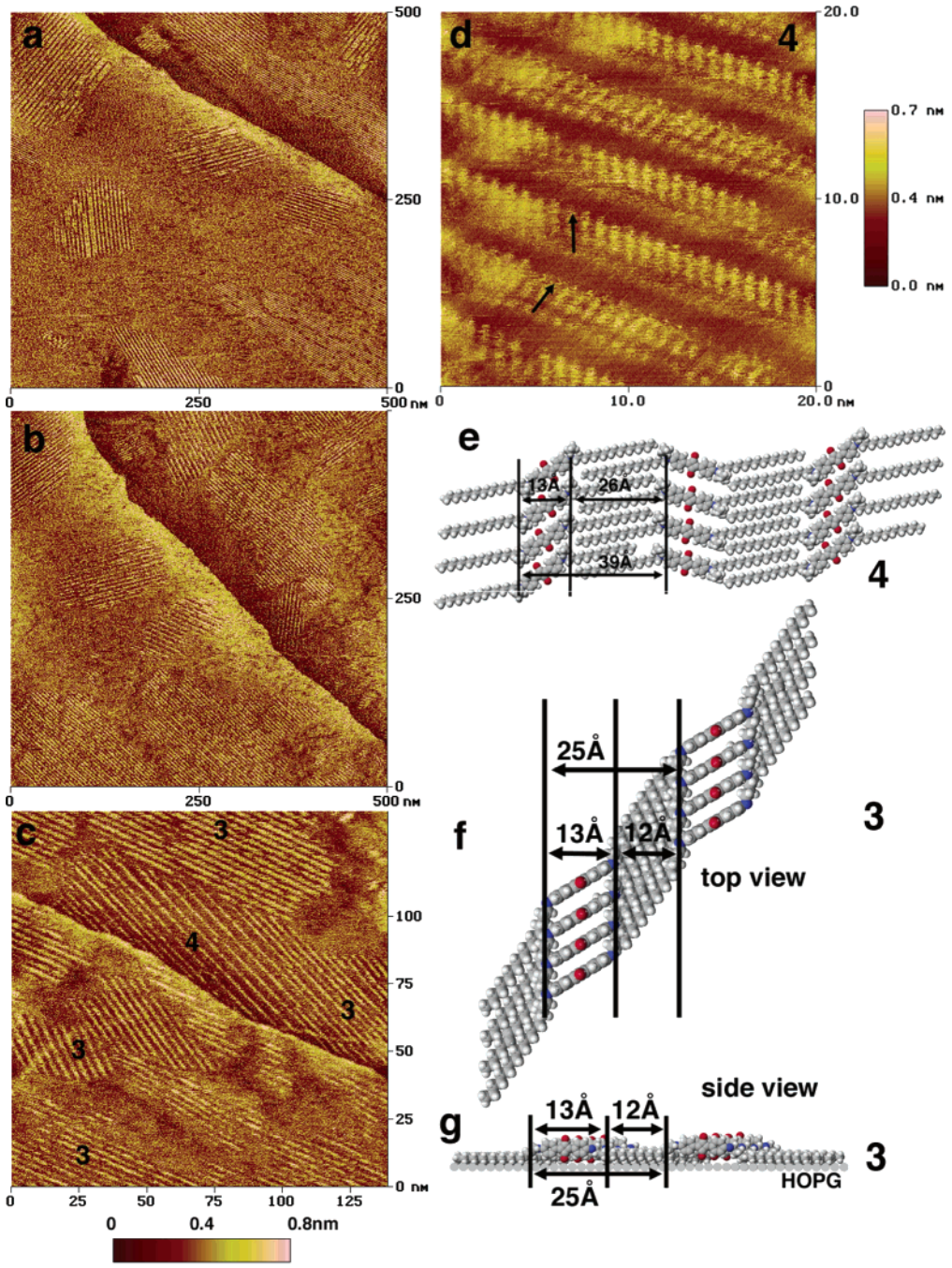

Figure 4. (a) 500 nm × 500 nm STM image showing nucleation of isolated ordered domains of 18-18HSQ amidst disordered adsorbate taken within 1 min of low concentration solution deposition. (b) Image of the same area of the surface taken 4 min later. (c) 135 nm × 135 nm image zoomed-in from image b showing domains of polymorphs 3 and 4. Disordered material and pinhole defects are visible between the domains. (d) 20 nm × 20 nm STM image of polymorph 4. Arrows overlaid on the image indicate the orientation of the chromophores within molecular rows. (e) Proposed single-layer molecular model of polymorph 4. (f) Top and (g) side view molecular models of the proposed single-layer card-stack conformation of polymorph 3.

Figure 4e illustrates this 2D single-layer structure. The incomplete interdigitation increases the effective width of the area occupied by tails beyond the ~20 Å length of an all-trans octadecyl tail. Unlike polymorph 2, however, the interdigitation is complete enough to preclude the adsorption of the remaining two octadecyl tails. For this reason, the remaining tails are shown protruding from the plane of the molecule in the model in Figure 4e. Since the alkyl tails are not resolved, it is also possible that the remaining tails are lying on top of the adsorbed tails. Black arrows overlaid on the image in Figure 4d point out another intriguing characteristic of this polymorph: the ability of the chromophores within a row to switch orientation from one row to the next (~60° to the direction of the row to ~120° in the next row, or vice versa). The splayed "z" shape of the proposed molecular surface structure of 18-18HSQ is 2D chiral since a molecule and its mirror image cannot be superimposed when rotated within the plane. STM images have previously resolved 2D enantiomers of several achiral molecules adsorbed on surfaces.[66,73−75] As illustrated in the molecular model in

(73) DeFeyter, S.; Grim, P. C. M.; Rucker, M.; Vanoppen, P.; Meiners, C.; Sieffert, M.; Valiyaveettil, S.; Mullen, K.; DeSchryver, F. C. *Angew. Chem., Int. Ed.* **1998**, *37*, 1223−1226.

(74) Yablon, D. G.; Giancarlo, L. C.; Flynn, G. W. *J. Phys. Chem. B* **2000**, *104*, 7627−7635.

Table 1. Structure of 18-18HSQ and Distance Parameters for the Four Main Polymorphs Exhibited by 18-18HSQ under Phenyloctane on HOPG as Measured with STM

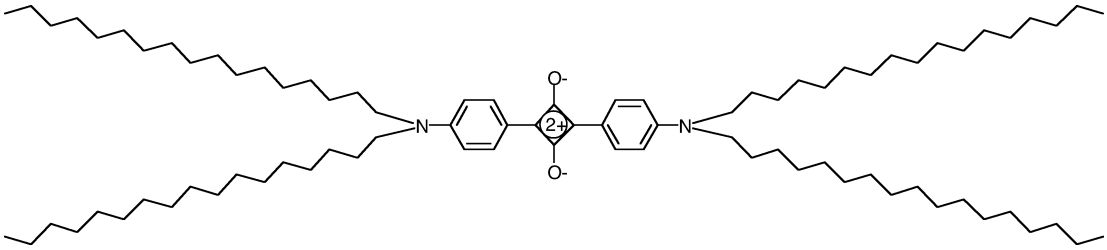

18-18HSQ polymorph	no. of layers in structure	bright row width (Å)	dark row width (Å)	*a* unit cell parameter (Å)
1	2	19 ± 2	13.5 ± 2.5	32 ± 2
2	2	16.5 ± 1.5	34 ± 3	50 ± 2
3	1 or 2	13 ± 1	12 ± 3	25 ± 1
4	1	13 ± 2	26 ± 3	39 ± 1

Figure 4e, the difference between 18-18HSQ molecules in rows with different chromophore orientations is determined by which pair of tails is adsorbed.

Polymorph 3 has a bright row width of 13 ± 1 Å and a dark row width of 12 ± 3 Å. As previously discussed, 13 Å is close to the length of a single 18-18HSQ chromophore; however, 12 Å is just over half the length of an octadecyl tail. If the 18-18HSQ molecules were to lie flat on the HOPG surface (as is observed for all other squaraines studied thus far on HOPG),[65,66] this would require either that the tails fold over on themselves (resulting in an apparent length of half of the all-trans length) or that they lie across the top of the chromophores making up the bright rows. Another possible explanation, that would allow the majority of the methylene units in the dodecyl tails to lie flat on the surface, is that the chromophores stand on edge, perpendicular to the HOPG surface, in a face-to-face card-stack fashion. This packing model is shown in Figure 4f,g. Figure 4f presents a top view of the structure, showing the face-to-face donor−acceptor interaction between adjacent chromophores laterally offset from one another (∼4 Å) within a card-stack aggregate. As was mentioned earlier, no solid-state crystal structures for 18-18HSQ have been reported. However, a solid-state structure with molecular packing similar to this card-stack model was reported by Wingard for bis(4-(dimethylamino)-2-methylphenyl) squaraine.[76] He found the interplanar distance to be ∼3.5 Å between adjacent face-on chromophores. In Law's review of the solid-state structures of several short-tailed aminophenyl squaraines, it was concluded that the C2 substituent in the phenyl ring has very little effect on the intermolecular charge transfer.[77] Therefore, it is reasonable to assume that 18-18HSQ could also exhibit the same chromophore−chromophore interaction despite the large difference in tail lengths. The side view of the model (Figure 4g) shows the relationships of the 18-18HSQ chromophore and tails to the HOPG surface. Two tails from each molecule (as is usual for row structures) are shown in direct contact with the HOPG surface. A few gauche defects in the first few carbons are necessary to allow this tail conformation. The rest of the tail may lie flat and have an attractive interaction with the surface. As shown in Figure 4f, the ends of the tails may interdigitate with the edge-on chromophores in the ∼3.5 Å of space between chromophores. In this way, all of the tails (excepting the first few methylene units) can interact with the surface. The two tails not in contact with the HOPG may interact with the tails on the surface by lying on top of them (again necessitating the incorporation of a few gauche defects). The resulting structure has the possibility of enjoying a strong chromophore−chromophore interaction as well as significant tail−graphite and tail−tail interactions. If the molecules are indeed adsorbed in a perpendicular card-stack, then high-resolution images should reveal the chromophores as thin lines 1−2 Å in width and ∼15 Å in length, with intralamellar chromophore distances of 3−4 Å. Rather, if they are adsorbed flat on the HOPG surface, then high-resolution images should reveal the chromophores as bright ellipses 4−5 Å in width. Adequate resolution to validate either of these models was not achieved, however. Table 1 summarizes all the measurements obtained for the four polymorphs.

High-Concentration Studies. Figure 5 shows two 500 nm × 500 nm STM images of the ordered adsorption from higher concentrations of 18-18HSQ in phenyloctane onto the graphite surface. The image in Figure 5a was taken a few seconds after solution deposition and shows a myriad of small (tens of nanometers to 100 nm in length or width) domains oriented predominantly at angles of 30° or multiples of 30° from one another. This angular dependence suggests an interaction along particular surface vectors of the graphite surface. Figure 5b shows an image taken during the same experiment (but in a different location on the graphite surface) a few hours after deposition. It is clear that the domains are much larger now with many of the domains being several hundred nanometers long. The elongated shape of the domains in Figure 5b indicates that for most of the nuclei, growth has occurred along the row direction. A 100 nm × 100 nm zoomed-in portion of Figure 5a, taken 5 min after the image in Figure 5a, is shown in Figure 6.

Several domains oriented close to 90° angles to one another are observed. Within these domains, an incredibly rich system of rows with varying apparent heights is observed. (This may be not a true topographical height but a convolution of electronic and topographical effects complicated by different possible electron paths through chromophores. The true topographical height is expected to be larger since it would be the thickness of a squaraine molecule.) Careful inspection reveals that there are four apparent row heights exhibited within this image that we will term (i) bright, (ii) medium, (iii) dim, and (iv) dark. These designations can be related to the *z*-scale bar, with (i) occurring highest on the bar, (iv) lowest, and (ii) and (iii) in between. This point is further illustrated by taking a cross section of a cluster of rows within the image (designated by a red line in Figure 6) that exhibits all four

(75) DeFeyter, S.; Gesquiere, A.; Wurst, K.; Amabilino, D.; Veciana, J.; DeSchryver, F. *Angew. Chem., Int. Ed.* **2001**, *40*, 3217−3220.
(76) Wingard, R. E. *IEEE Trans. Ind. Appl.* **1982**, 1251−1254.
(77) Law, K. Y. *Chem. Rev.* **1993**, *93*, 449−486.

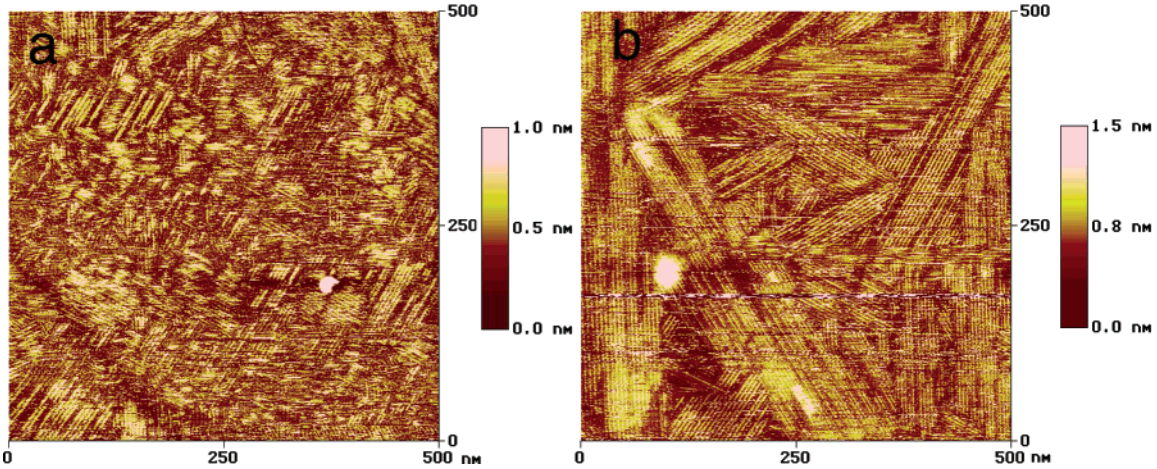

Figure 5. (a) 500 nm × 500 nm image taken a few seconds after deposition of a high-concentration 18-18HSQ solution onto the HOPG surface. Many small domains are shown covering the surface, oriented at predominantly 30° angles to one another. (b) 500 nm × 500 nm image taken 4 h after image a on a different area of the same surface.

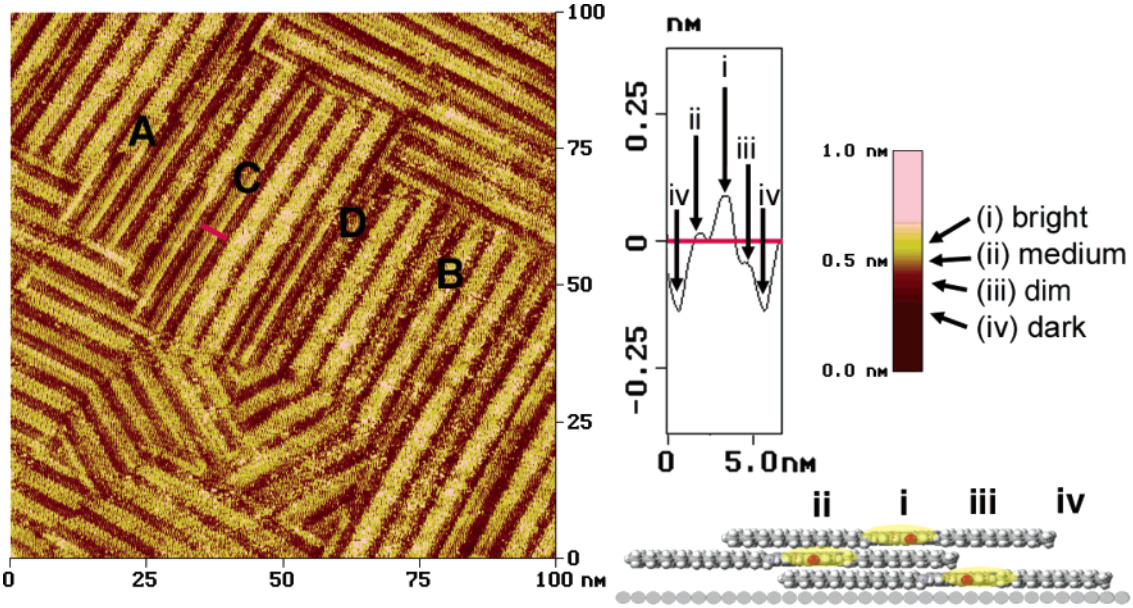

Figure 6. (Left) 100 nm × 100 nm image showing several domains at 90° or 120° to one another, displaying rows of four different contrasts: (i) bright, (ii) medium, (iii) dim, and (iv) dark. These contrast designations can be related to different apparent heights, illustrated by the scale bar and the image cross section. The red line indicates the cluster of rows in the image from which the section is taken. A molecular model of this cross section appears below on the right. The observed image contrasts (i), (ii), (iii), and (iv) are overlaid on their corresponding areas within the model. Chromophores are highlighted in yellow. Letters overlaid on the image illustrate the four variations of row clusters: type A (i)/(i)/(i), type B (i)/(i)/(iii), type C (ii)/(i)/(iii), and type D (ii)/(ii)/(iii).

apparent row heights. It can clearly be seen that the bright row (i) has the largest apparent height, the medium contrast row (ii) has the next largest height, the dim row (iii) has the third largest height, and the dark row (iv) appears as a trough. The difference between the apparent heights of the bright and medium rows ((i) and (ii)), the medium and dim rows ((ii) and (iii)), and the dim and dark contrast rows ((iii) and (iv)) is ∼1 Å for each pairing (within error of the measured height of a squaraine chromophore in previous STM studies).[65,66,78] The width of each of the rows (measured perpendicular to the edge of the row) was also consistently 12 ± 1 Å for (i), (ii), and (iii). The ∼12 Å width corresponds well with the length of a squaraine chromophore. Dark rows (iv) were slightly narrower at 8.5 ± 1.5 Å. The similarity of the measured row widths to the squaraine chromophore length and the consistent differences in apparent heights between the rows of differing contrast lead us to believe that each of the different heights (except the dark rows) corresponds to a different layer of chromophores in the multilayer. The film shown in Figure 6 then consists of at least three layers of 18-18HSQ molecules. The dim rows (iii) correspond to chromophores that are in contact with the HOPG surface (the bottom or first layer); the medium height rows (ii) are adsorbed atop the first layer (the middle or second layer); and the bright rows (i) are the top (or third) layer.

Assuming an adsorbate-mediated tunneling mechanism (resonant tunneling from the tip into an adsorbate state with subsequent resonant tunneling into a substrate state), this particular designation of image contrast with layer identity (i.e., bright contrast with the layer furthest from the HOPG surface) seems counterintuitive. Adsorbate-mediated tunneling (a tunneling mechanism involving alteration of the surface electronic states by an adsorbate) would necessitate that the adsorbate being

(78) Takeda, N.; Stawasz, M. E.; Parkinson, B. A. *J. Electroanal. Chem.* **2001**, *498*, 19−33.

imaged be in close proximity to the surface. Since tunneling current decays exponentially with distance, one may expect that adsorbate layers closest to the substrate surface exhibit the highest tunneling current and thus brightest image contrast. Likewise, the greatest adsorbate−substrate electronic state mixing would occur between the substrate and the molecules adsorbed in the proximal layer. We presume, however, that the molecular contrast of the squaraine system occurs by another tunneling mechanism that likely incorporates their ability to undergo intermolecular charge transfer.[64,76,77,79−84] The details of this mechanism will not be presented here but were discussed in a previous paper.[65]

Closer examination of the varying apparent heights ((i), (ii), (iii), and (iv)) exhibited by the rows in Figure 6 reveals several patterns. Dark rows (iv), or troughs, occur approximately every fourth row. Thus, (i), (ii), and (iii) rows appear to cluster in groups of three. The contrast sequences within these clusters display four different combinations: (A) (i)/(i)/(i), (B) (i)/(i)/(iii), (C) (ii)/(i)/(iii), and (D) (ii)/(ii)/(iii). To facilitate recognition of each type of cluster within the image, the letter of each of the four cluster types is overlaid on the image in Figure 6 in a region displaying each type. Figure 7 shows a zoomed-in portion of Figure 6 (a) and cross sections (b) of each of the four cluster types.

The red and blue lines overlaid on the image show where the cross sections were taken. Again, the letter of each of the clusters is overlaid on both the image (where the cross sections were taken) and the cross sections themselves. In addition, the apparent height of each of the rows within each cluster is designated by (i), (ii), (iii), or (iv) in the cross section. As was mentioned earlier, the consistency in the differences in apparent height (∼1 Å) and the similarity in size of the widths of the (i), (ii), and (iii) rows (∼12 Å) with the length of a squaraine chromophore lead us to believe that the (i), (ii), and (iii) rows are lamellae of squaraine chromophores in the bottom (iii), middle (ii), and top (i) layers of a three-layer film.

The following analysis attempts to discern the polytype of the ordered structures in each of the layers. The distance from the left edge of a cluster of rows to the left edge of the nearest cluster is consistently ∼50 Å, regardless of the contrast sequences of the neighboring clusters. The same is true for the distance from the second row of a three-row cluster to the second row of its neighboring three-row cluster and the distance from the right edge to the next cluster's right edge. Thus it appears that the single-layer structure of each of the three layers has the same *a* unit cell parameter of 50 Å. Recall that polymorph 2 of the low concentration solution structures presented earlier also exhibits a 50 Å *a* unit cell parameter. Polymorph 2, however, exhibits a bright row width of ∼17 Å and consists of a two-layer structure in which the chromophores in adjacent layers overlap by ∼7 Å. It is clear in the clusters shown in Figure 7a that the chromophores of adjacent layers do not overlap: they appear distinctly and separately as ∼12 Å wide rows. Although the combined two-layer structure of polymorph 2 is not the same as that observed here, it is likely that the single-layer structure of polymorph 2 (its first layer) and the thin films shown here are similar, if not the same.

As mentioned earlier, the chromophores in polymorph 2 were not resolved and thus the actual angle of the chromophores within a molecular row to the direction of the row was not determined. As a result, the model for polymorph 2 (Figure 3b,c) was constructed using a molecular angle that had been found to be common for other long-tailed squaraine systems (50°). Unlike the low-concentration studies, single-molecule resolution was achieved in Figure 7a in some of the bright (i) and medium (ii) apparent height rows and allowed measurement of the angle of the chromophores to the direction of their molecular row. It was found to be ∼50° for both row apparent heights ((i) and (ii)) in this system. Although it could not be resolved, it is assumed that a similar angle exists in the dim (iii) apparent height rows. As a result of this common molecular angle and *a* unit cell parameter, the single-layer structure used to construct the models of the multiple-layer films observed here was the same as that used in the low-concentration polymorph 2.

Figure 7c−f show top and side views of the proposed models for the (c) type C (ii)/(i)/(iii), (d) type D (ii)/(ii)/(iii), (e) type B (i)/(i)/(iii), and (f) type A (i)/(i)/(i) row clusters. To facilitate recognition of the three-row cluster region in the models, red vertical lines enclose the cluster region. In the side views of the models, the rows of chromophores within the cluster region are highlighted in yellow. They are further labeled with their observed STM image contrast, (i), (ii), (iii), or (iv). As mentioned above, each of the molecular layers within each cluster type is assumed to have the same or similar structure, that is represented by the first layer of the polymorph 2 structure. This structure is shown in its entirety as the bottom (shadowed) layer in the top view of each of the models. Except for model d, only the chromophore region of the molecules is shown in the subsequent layers. The tails are left out of the top view of the model in these layers for two reasons: (1) to facilitate viewing of the interlayer relationship of the chromophores and (2) because the tails do not contribute to the tunneling contrast in the STM images of these cluster structures. As can be seen in the top view, the chromophores of subsequent layers do not overlap in any of the cluster types; either they are separate and discreet or they are totally eclipsed by the chromophore of a subsequent layer. This is surprising considering that the low-concentration multilayer polymorphs (and multilayer polymorphs of other squaraines) each included substantial donor−acceptor interactions between molecules in adjacent layers.[65] Instead, in these cluster models the chromophores of each subsequent layer adsorb atop the tail region of the layer beneath them. This can be seen in the side views of the models, which include the tails for all the molecular layers in each of the cluster types.

The type C cluster of rows ((ii), (i), (iii)), shown in Figure 7c, is the only cluster in which all three of the molecular layers are resolved. Each row in the STM image (Figure 7a) appears to be adjacent to a row of a different apparent height. However, since the adjacent rows have different apparent heights, the chromophores of each of the rows are actually in different layers. As a result, there is no steric hindrance between the adjacent (i) and (ii) and (i) and (iii) rows, so that the tails of the molecules within each of the layers may lie flat and interact with the adjacent tails both within their own layer and in the adjacent layer(s).

The remaining cluster types involve adjacent rows of the same contrast: type D (ii)/(ii)/iii), type B (i)/(i)/(iii), and type A (i)/(i)/(i). The proximity of the adjacent

(79) Loutfy, R. O.; Hsiao, C. K.; Kazmaier, P. M. *Photogr. Sci. Eng.* **1983**, *27*, 5−9.
(80) Bernstein, J.; Tristani-Kendra, M.; Eckhardt, C. J. *J. Phys. Chem.* **1986**, *90*, 1069−1073.
(81) Tristani-Kendra, M.; Eckhardt, C. J.; Bernstein, J.; Goldstein, E. *Chem. Phys. Lett.* **1983**, *98*, 57−61.
(82) Tristani-Kendra, M.; Eckhardt, C. J. *J. Chem. Phys.* **1984**, *81*, 1160.
(83) Law, K. Y. *J. Phys. Chem.* **1987**, *91*, 5184−5193.
(84) Law, K. Y.; Facci, J. S.; Bailey, F. C.; Yanus, J. F. *J. Imaging Sci.* **1990**, *34*, 31−38.

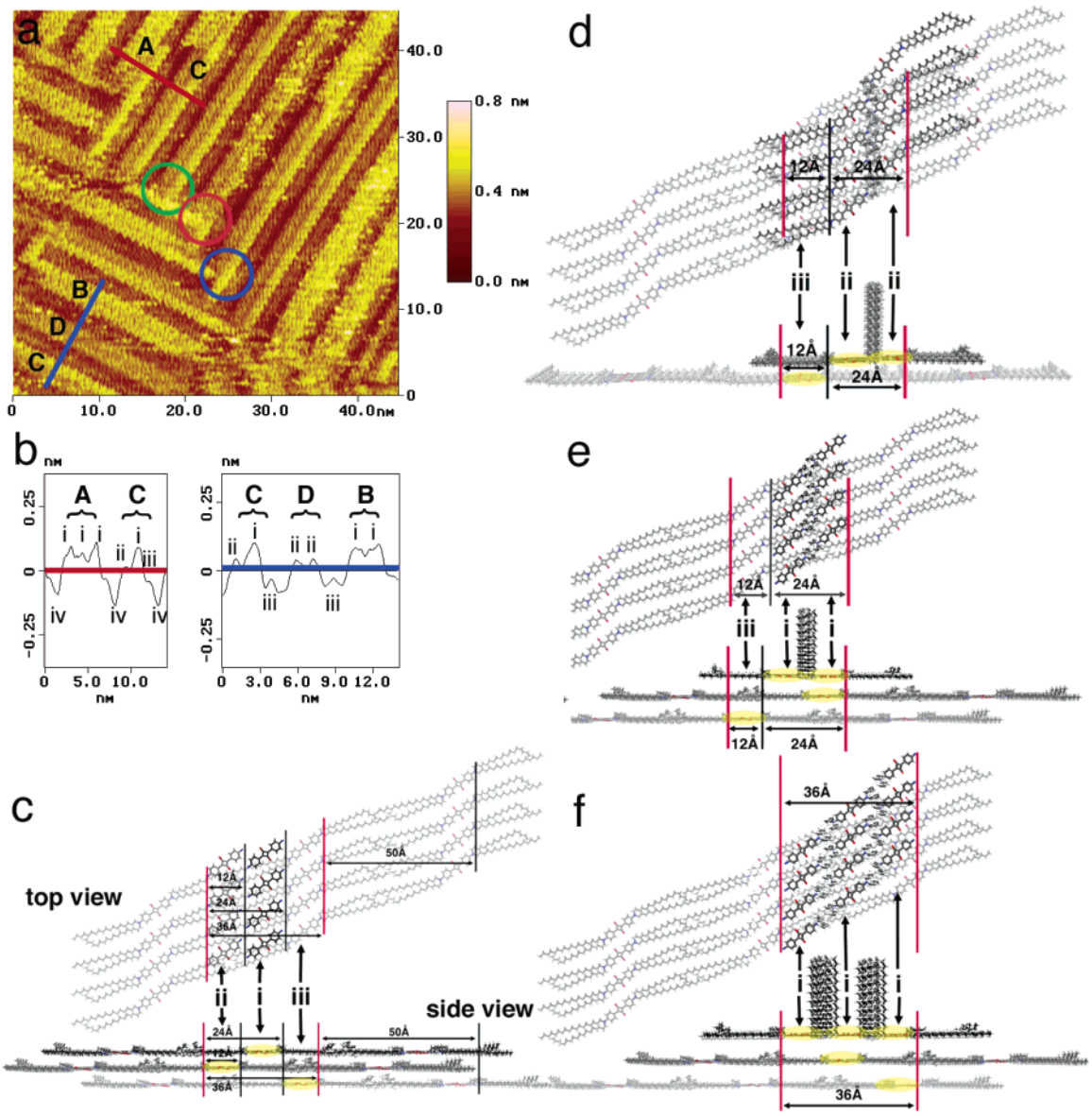

Figure 7. (a) 45 nm × 45 nm image zoomed-in from Figure 6 exhibiting the four cluster types: type A (i)/(i)/(i), type B (i)/(i)/(iii), type C (ii)/(i)/(iii), and type D (ii)/(ii)/(iii). Red and blue lines overlaid on the image correspond to the cross sections (b) of the same color below. Letters overlaid on the image and on the cross sections designate the cluster type shown. The cross sections illustrate the differences in apparent height between the bright (i), medium (ii), dim (iii), and dark (iv) contrast rows and the sequences of these row heights for each cluster. (c−f) Top and side views of the proposed three-layer molecular models of the (c) type C, (d) type D, (e) type B, and (f) type A clusters. The layers for each cluster have the same polymorph 2 structure; however, the tails are left out of the models of the second (middle) and third (top) layers in the three-layer models for simplicity. The first (bottom) layer is shown in its entirety in the top view in muted contrast. The middle layer is shown as medium contrast, while the top layer is the darkest row of chromophores. The side view shows the entire structure of all two (d) or three (c,e,f) of the layers. The chromophores are highlighted in yellow to facilitate recognition. Chromophore regions in both the top and side views of the cluster models are labeled with their observed STM image contrast. The regions of the models that correspond to the clusters observed in image a are bracketed by red lines. Red, blue, and green rings overlaid on image a designate three types of 90° row intersections: 90° turn, T intersection, and false T intersection, respectively.

molecular rows of the same apparent height complicates the cluster structure. Molecular rows of the same apparent height are in the same layer. This proximity precludes the inclusion of the alkyl tails in the plane of the molecule in the region between adjacent chromophores of the same apparent height. As a result, we have modeled the tails in this intermolecular region as oriented perpendicular to the plane of the chromophore. This can be seen in Figure 7d in the model for the type D cluster ((ii)/(ii)/(iii)), where a single row of perpendicular tails can be seen. (We refer to the perpendicular tails in this inter-row region as a single "row" of tails despite the fact that the tails are actually from two different molecular rows. The singularity in the term "row" comes from the single inter-row region that all of the tails occupy. Two rows would then indicate two inter-row regions of perpendicularly oriented tails.) This tail orientation allows the chromophores in adjacent rows to get close enough together to achieve the 24 Å total (ii)/(ii) row distance measured. In addition, as can be seen in the side view of the model, this orientation allows attractive dispersion interactions between the vertically oriented tails. The total attractive interaction between the tails may mitigate any molecule−molecule repulsion between the amino groups of adjacent molecules, thus allowing chromophores to orient end to end. Also, adventitious water may exist in some structures and

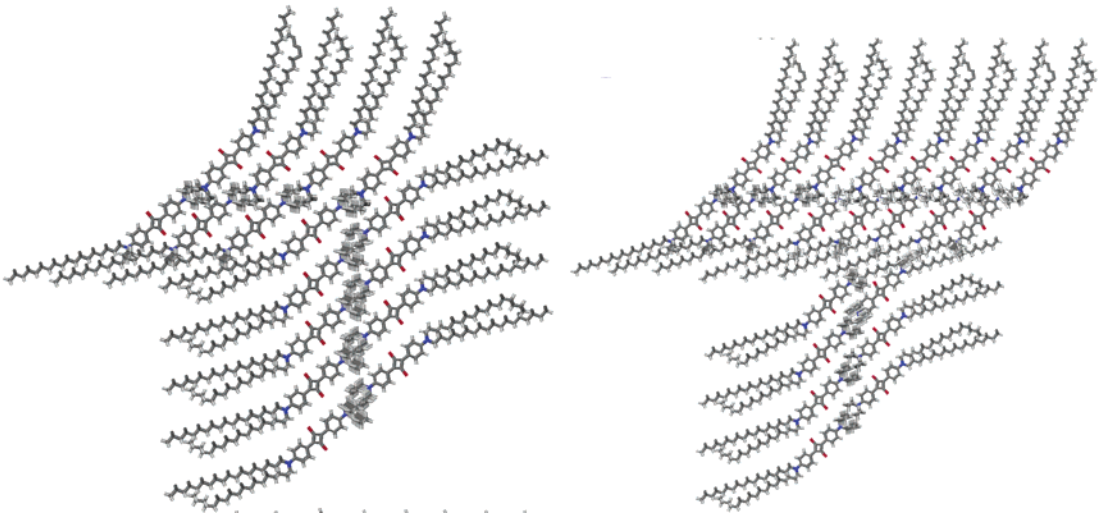

Figure 8. Models of the 90° turn (left) and T intersection (right) corresponding to the row intersections in Figure 7a designated by the red and blue rings.

contribute to H-bonding between molecules. Figure 7e shows the model for the type B, (i)/(i)/(iii), row cluster. From the top, the (i)/(i)/(iii) model looks the same as the (ii)/(ii)/(iii), type D, model. However, as can be seen in the side view, it is actually composed of three layers, the second layer of which is eclipsed by the third (top) layer. Chromophores in the top layer appear as bright (i) apparent height rows, those in the bottom layer appear as dim (iii) rows, and the middle layer chromophores do not appear at all because they are eclipsed by the top layer. Like the (ii)/(ii)/(iii) clusters, the tails in rows adjacent to another row of the same contrast are shown perpendicular to the molecular plane. The (i)/(i)/(i) row cluster structure (type A) is similar to that of the (i)/(i)/(iii) type B cluster. Figure 7f shows the proposed model for the (i)/(i)/(i) structure, which is identical to that in Figure 7e with the addition of a third consecutive row in the topmost (third) layer, producing a total of two rows of perpendicular tails.

In addition to exhibiting the remarkable multiple-layer row clusters mentioned above, the molecular layers shown in Figure 7a also reveal intriguing 90° angles between adjacent domains, apparently incompatible with the hexagonal symmetry of the HOPG substrate. At least three types of 90° intersections can be observed in the image shown in Figure 7a. Each type is highlighted with a different color ring. The first type, indicated by a red ring, exhibits a row of a particular apparent height suddenly taking a 90° turn, merging into a row of the same apparent height in an adjacent domain oriented 90° to the first domain. As shown in the model in the left side of Figure 8, if the chromophores within a row are oriented ∼45° to the edge of the row, then the orientation of a chromophore in a row 90° to the first is practically indistinguishable from that of the chromophores in the first row.

Therefore, the same intermolecular interaction is possible between two adjacent chromophores in rows oriented 90° to one another compared to that between two chromophores in the same row. As a result, a row (or pair of rows) may make a 90° turn. This is exemplified by the frequent occurrence of 90° turns in rows of both medium (ii) and bright (i) contrast. A second type of 90° intersection, indicated in Figure 7a by a blue ring, resembles a "T". In this type, a row of a particular contrast appears to be capped or abruptly interrupted by a row of the same contrast oriented 90° to it. Close inspection of these areas shows that a slight gap exists between most 90° rows involved in T intersections. Therefore, unlike the 90° turn, the perpendicular molecular rows do not connect. We interpret this gap to signify that there is no chromophore−chromophore interaction between the rows at 90° to one another in this T conformation. A model of this structure is shown in the right side of Figure 8. If the rows comprising the T intersection actually met one another, as they do in the 90° turn, the intersection area would result in a large amount of steric hindrance due to the abundance of tails in this intersection region. In addition, the chromophores at this intersection would have to overlap, thus creating a difference in apparent height between the overlapping chromophores. The two intersection types just described occur between rows of the same apparent height that intersect at 90° angles. A third type of 90° intersection (indicated in Figure 7a by a green ring) can be observed between rows of differing contrast (medium and bright rows) oriented perpendicular to one another. This type of intersection is always located next to a 90° turn or T intersection. In this intersection, one of the rows appears to abruptly end at a perpendicular row. With the exception that the intersecting rows differ in apparent height, it appears to be a T intersection. But the fact that the intersecting rows are of different contrasts, signifying that they are in different layers, indicates that the rows do not intersect in the same plane but are only overlapping at 90°. Therefore, it is not a true intersection.

Some high-concentration experiments did not produce the row clusters with the 90° intersections just described. Instead, small domains similar to that in Figure 5a composed primarily of polymorph 1 were observed. These domains grew across the surface until they covered the HOPG. When the HOPG was covered, growth continued in a layer-by-layer fashion (although not in the layered structures just discussed). An example of the layer-by-layer growth is shown in the time-lapse sequence of images in Figure 9a−c. The image in Figure 9a was captured 12 min after solution deposition and shows a fairly complete adsorbed layer of polymorph 1 with rows oriented ∼110° to the left edge of the image. Faintly visible rows of different orientations are seen growing in on top of this layer. Image b, captured 23 min after image a, clearly shows the growth of the second layer forming a cross-hatched pattern over the still-visible first layer. The predominant orientation of the second-layer domains is 60/120° to the orientation of the first layer, although some adsorption is occurring on top of the first layer in the

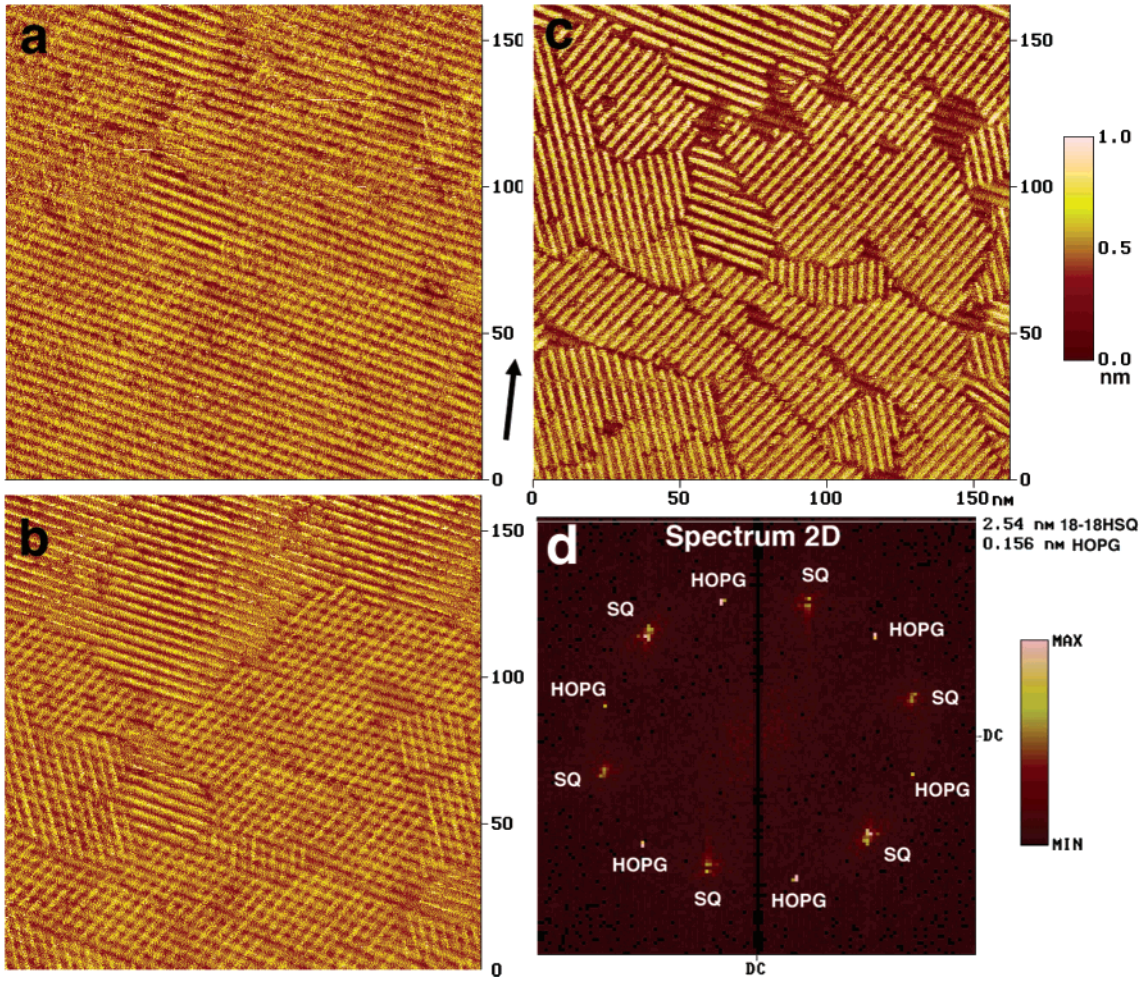

Figure 9. (a−c) Three 160 nm × 160 nm images showing the same area, taken over a period of 32 min showing the growth of multiple layers of adsorbed 18-18HSQ. Image a was taken 12 min after solution deposition, image b was taken 23 min after image a, and image c was taken 9 min after image b. The black arrow shows the direction of image drift. (d) Overlaid 2D Fourier spectra of HOPG and the 18-18HSQ overlayer shown from image c. Spots corresponding to the overlayer and the substrate lattices are labeled by either HOPG or SQ. The Fourier spectra are normalized in intensity and distance, but the angular relationship has not been altered. 18-18HSQ spots appear 30° from the HOPG spots, illustrating an orientational relationship between the overlayer and the substrate.

same orientation as the first layer. Figure 9c, captured 9 min after image b, shows a more complete second layer with the first layer now only visible in small patches.

Epitaxial Relationship of 18-18HSQ with HOPG. As mentioned in previous sections, domains of 18-18HSQ tend to orient with respect to one another at angles that are multiples of 30°. These orientations signify an epitaxial relationship of the domain directions with the underlying HOPG substrate. When domain directions were compared to the directions of the underlying HOPG, a 30° difference was often found between the orientations of the domains (row directions) and the orientation of the HOPG lattice. This is illustrated in Figure 9d where the 2D Fourier spectrum of the image shown in Figure 9c and that of the HOPG lattice are overlaid. The image shown in Figure 9c contains several domains of polymorph 1. The image of the HOPG surface from which the other spectrum was taken (not shown) was captured 5 min after the squaraine image on the same area of the surface. The overlaid spectra were normalized in both intensity and magnification to emphasize orientation only. The spots for HOPG and 18-18HSQ rows within the spectrum are labeled. It is evident that both the HOPG and the domain directions of the 18-18HSQ overlayer have 3-fold symmetry. It is also clear that the 18-18HSQ spots occur 30° from the HOPG spots, indicating that the squaraine overlayer has a coincident relationship to the HOPG lattice. The comparison of 2D Fourier spectra for 18-18HSQ overlayers and HOPG was not achieved for all polymorphs; however, many domains exhibited orientation angles that varied by multiples of 30°, a relationship that reflects the symmetry of the HOPG lattice. It appears that the polymorphs observed for 18-18HSQ on HOPG have a stronger epitaxial relationship to HOPG than any of the previously studied squaraine layers on HOPG.[65,66]

Conclusions

We have reported the nucleation and growth of ordered layers of 18-18HSQ, from phenyloctane solutions containing both low and high concentrations of the squaraine, onto the basal plane of HOPG. The large number of polymorphs observed for this molecule on HOPG is common for long-tailed squaraines. A total of seven polymorphs, many with complex multiple-layer structures, were observed for the adsorption of 2-18OHSQ on HOPG from phenyloctane solutions.[65] The large number of observed polymorphs for these two molecules (2-18OHSQ and 18-18HSQ), as compared to the number for shorter-tailed squaraines,[65,66] is probably due to the large number of attractive methylene−methylene dispersion interactions between octadecyl tails and the variety of ways that these interactions may occur. Attractive tail−tail interac-

tions may arise between (1) the alkyl tails of molecules in adjacent rows within the same molecular layer through interdigitation; (2) the alkyl tails of molecules in adjacent layers, through stacking; and (3) the two alkyl tails on the same side of a single molecule through gauche defects that allow both of the tails to reside in or near the surface plane. Additionally, the large number of attractive methylene−methylene interactions allows for small variations in the total energy of these interactions. As a result, numerous structures may be formed with similar energies. Although the alkyl tails interacting with the HOPG probably drive the formation of the row structures, the intralayer chromophore−chromophore interactions, similar to those exhibited by other squaraines adsorbed on HOPG, were still present in all of the ordered structures.

Adsorbed 18-18HSQ forms at least four polymorphs, three of which are multiple-layer structures. Single-layer polymorphs were observed only at low concentrations; however, multiple-layer structures were observed at both low and high concentrations immediately following solution deposition onto the HOPG. The single-layer polymorph also showed 2D chirality due to the splayed "z" shape of the molecule on the surface. One polymorph is probably the thermodynamically most stable structure, but without performing extended time and/or temperature studies, we cannot identify the most stable polymorph.

Many of the polymorphs exhibited a coincident relationship to the HOPG surface since domain angles were most often multiples of 30°. Remarkable multiple-layer films may be formed from the layering of two-layer polymorphs onto one another. Interlayer chromophore−chromophore interactions were sometimes not present between the multiple layers. The conductivity of the squaraine molecules and the relatively low tunneling currents used allowed the imaging of many layers of 18-18HSQ molecules on the HOPG surface, something that is not often seen in STM imaging of molecular layers.

The models presented for the structures presented herein are probably not unique and are not meant to be definitive. Other structural models can be imagined that will also fit the data obtained from the STM images. This is at least partially due to the fact that perfect submolecular resolution is not always achieved and perhaps is not possible in multilayer structures such as those postulated herein. Nonetheless, we believe that our postulated structures are a valid attempt at understanding the complex surface structures and will perhaps give guidance to future work on the transition of monolayer structures of surface-active molecules into thick films and eventually bulk structures.

Acknowledgment. We thank Dr. Marina Stanescu of the Whitten group at the University of Rochester for supplying us with bis(4-dioctadecylamino-phenyl) squaraine (18-18HSQ). This work was supported by the Department of Energy, Office of Basic Energy Sciences, under Contract DE-F603-96ER14625.

LA035238Q